

## Final reports of the Stardust Interstellar Preliminary Examination

Andrew J. WESTPHAL<sup>1\*</sup>, Hans A. BECHTEL<sup>2</sup>, Frank E. BRENKER<sup>3</sup>, Anna L. BUTTERWORTH<sup>1</sup>, George FLYNN<sup>4</sup>, David R. FRANK<sup>5</sup>, Zack GAINSFORTH<sup>1</sup>, Jon K. HILLIER<sup>6</sup>, Frank POSTBERG<sup>6</sup>, Alexandre S. SIMIONOVICI<sup>7</sup>, Veerle J. STERKEN<sup>8,9,10</sup>, Rhonda M. STROUD<sup>11</sup>, Carlton ALLEN<sup>12</sup>, David ANDERSON<sup>1</sup>, Asna ANSARI<sup>13</sup>, Saša BAJT<sup>14</sup>, Ron K. BASTIEN<sup>5</sup>, Nabil BASSIM<sup>15</sup>, Janet BORG<sup>16</sup>, John BRIDGES<sup>17</sup>, Donald E. BROWNLEE<sup>18</sup>, Mark BURCHELL<sup>19</sup>, Manfred BURGHAMMER<sup>20</sup>, Hitesh CHANGELA<sup>21</sup>, Peter CLOETENS<sup>20</sup>, Andrew M. DAVIS<sup>22</sup>, Ryan DOLL<sup>23</sup>, Christine FLOSS<sup>23</sup>, Eberhard GRÜN<sup>24</sup>, Philipp R. HECK<sup>25</sup>, Peter HOPPE<sup>26</sup>, Bruce HUDSON<sup>27</sup>, Joachim HUTH<sup>26</sup>, Brit HVIDE<sup>13</sup>, Anton KEARSLEY<sup>28</sup>, Ashley J. KING<sup>29</sup>, Barry LAI<sup>30</sup>, Jan LEITNER<sup>26</sup>, Laurence LEMELLE<sup>31</sup>, Hugues LEROUX<sup>32</sup>, Ariel LEONARD<sup>23</sup>, Robert LETTIERI<sup>1</sup>, William MARCHANT<sup>1</sup>, Larry R. NITTLER<sup>33</sup>, Ryan OGLIORE<sup>34</sup>, Wei Ja ONG<sup>23</sup>, Mark C. PRICE<sup>19</sup>, Scott A. SANDFORD<sup>35</sup>, Juan-Angel Sans TRESSERAS<sup>20</sup>, Sylvia SCHMITZ<sup>3</sup>, Tom SCHOONJANS<sup>36</sup>, Geert SILVERSMIT<sup>36</sup>, Vicente A. SOLÉ<sup>20</sup>, RALF SRAMA<sup>37</sup>, Frank STADERMANN<sup>23</sup>, Thomas STEPHAN<sup>22</sup>, Julien STODOLNA<sup>1</sup>, Steven SUTTON<sup>30</sup>, Mario TRIELOFF<sup>6</sup>, Peter TSOU<sup>38</sup>, Akira TSUCHIYAMA<sup>39</sup>, Tolek TYLISZCZAK<sup>2</sup>, Bart VEKEMANS<sup>36</sup>, Laszlo VINCZE<sup>36</sup>, Joshua VON KORFF<sup>1</sup>, Naomi WORDSWORTH<sup>40</sup>, Daniel ZEVIN<sup>1</sup>, Michael E. ZOLENSKY<sup>10</sup>, and > 30,000 Stardust@home dusters<sup>41</sup>

<sup>1</sup>Space Sciences Laboratory, University of California, Berkeley, California, USA

<sup>2</sup>Advanced Light Source, Lawrence Berkeley Laboratory, Berkeley, California, USA

<sup>3</sup>Geoscience Institute, Goethe University Frankfurt, Frankfurt, Germany

<sup>4</sup>SUNY Plattsburgh, Plattsburgh, New York, USA

<sup>5</sup>ESCG, NASA JSC, Houston, Texas, USA

<sup>6</sup>Institut für Geowissenschaften, University of Heidelberg, Heidelberg, Germany

<sup>7</sup>Institut des Sciences de la Terre, Observatoire des Sciences de l'Univers de Grenoble, Grenoble, France

<sup>8</sup>IRS, University Stuttgart, Stuttgart, Germany

<sup>9</sup>IGEP, Technische Universität Braunschweig, Braunschweig, Germany

<sup>10</sup>MPIK, Heidelberg, Germany

<sup>11</sup>Materials Science and Technology Division, Naval Research Laboratory, Washington, District of Columbia, USA

<sup>12</sup>ARES, NASA JSC, Houston, Texas, USA

<sup>13</sup>Robert A. Pritzker Center for Meteoritics and Polar Studies, The Field Museum of Natural History, Chicago, Illinois, USA

<sup>14</sup>DESY, Hamburg, Germany

<sup>15</sup>Nanoscale Materials Section, Naval Research Laboratory, Washington, District of Columbia, USA

<sup>16</sup>IAS Orsay, Orsay, France

<sup>17</sup>Space Research Centre, University of Leicester, Leicester, UK

<sup>18</sup>Department of Astronomy, University of Washington, Seattle, Washington, USA

<sup>19</sup>University of Kent, Canterbury, Kent, UK

<sup>20</sup>European Synchrotron Radiation Facility, Grenoble, France

<sup>21</sup>George Washington University, Washington, District of Columbia, USA

<sup>22</sup>University of Chicago, Chicago, Illinois, USA

<sup>23</sup>Washington University, St. Louis, Missouri, USA

<sup>24</sup>Max-Planck-Institut für Kernphysik, Heidelberg, Germany

<sup>25</sup>Field Museum of Natural History, Chicago, Illinois, USA

<sup>26</sup>Max-Planck-Institut für Chemie, Mainz, Germany

<sup>27</sup>Midland, Ontario, Canada

<sup>28</sup>Natural History Museum, London, UK

<sup>29</sup>The University of Chicago and Robert A. Pritzker Center for Meteoritics and Polar Studies,  
The Field Museum of Natural History, Chicago, Illinois, USA

<sup>30</sup>Advanced Photon Source, Argonne National Laboratory, Chicago, Illinois, USA

<sup>31</sup>Ecole Normale Supérieure de Lyon, Lyon, France

<sup>32</sup>University Lille 1, Lille, France

<sup>33</sup>Carnegie Institution of Washington, Washington, District of Columbia, USA

<sup>34</sup>University of Hawai'i at Manoa, Honolulu, Hawai'i, USA

<sup>35</sup>NASA Ames Research Center, Moffett Field, California, USA

<sup>36</sup>University of Ghent, Ghent, Belgium

<sup>37</sup>IRS, University Stuttgart, Stuttgart, Germany

<sup>38</sup>Jet Propulsion Laboratory, Pasadena, California, USA

<sup>39</sup>Osaka University, Osaka, Japan

<sup>40</sup>South Buckinghamshire, UK

<sup>41</sup>Worldwide

\*Corresponding author. E-mail: westphal@ssl.berkeley.edu

(Received 19 December 2012; revision accepted 19 September 2013)

---

**Abstract**—With the discovery of bona fide extraterrestrial materials in the Stardust Interstellar Dust Collector, NASA now has a fundamentally new returned sample collection, after the Apollo, Antarctic meteorite, Cosmic Dust, Genesis, Stardust Cometary, Hayabusa, and Exposed Space Hardware samples. Here, and in companion papers in this volume, we present the results from the Preliminary Examination of this collection, the Stardust Interstellar Preliminary Examination (ISPE). We found extraterrestrial materials in two tracks in aerogel whose trajectories and morphology are consistent with an origin in the interstellar dust stream, and in residues in four impacts in the aluminum foil collectors. While the preponderance of evidence, described in detail in companion papers in this volume, points toward an interstellar origin for some of these particles, alternative origins have not yet been eliminated, and definitive tests through isotopic analyses were not allowed under the terms of the ISPE. In this summary, we answer the central questions of the ISPE: How many tracks in the collector are consistent in their morphology and trajectory with interstellar particles? How many of these potential tracks are consistent with real interstellar particles, based on chemical analysis? Conversely, what fraction of candidates are consistent with either a secondary or interplanetary origin? What is the mass distribution of these particles, and what is their state? Are they particulate or diffuse? Is there any crystalline material? How many detectable impact craters (>100 nm) are there in the foils, and what is their size distribution? How many of these craters have analyzable residue that is consistent with extraterrestrial material? And finally, can craters from secondaries be recognized through crater morphology (e.g., ellipticity)?

---

## STARDUST MISSION

Stardust, a NASA Discovery-class mission, was the first sample return mission to return solid samples from beyond the Moon. Stardust was effectively two missions carried on one spacecraft bus. The primary mission was to return solid samples from the Jupiter-family comet 81P/Wild 2. The second mission, to return the first solid samples from the contemporary interstellar dust stream, was considered to be “bonus” science for the purposes of mission planning. However, the scientific community considered this mission to be as important as the cometary one.

The Stardust Interstellar Dust Collector was exposed to the contemporary interstellar dust stream for

195 days in 2000 and 2002 (Figs. 1–3). The collector itself was composed of 132 aerogel tiles and 291 strips of aluminum foils, with total collecting areas of approximately 1039 cm<sup>2</sup> and approximately 150 cm<sup>2</sup>, respectively. In practice, the collecting area is reduced because of damaged margins of the aerogel tiles, the impracticality of completely intact extraction of foils from the collector, and other complications. An additional challenge has to do with the fact that the use of foils as a collecting medium is serendipitous—they were not originally intended for this use. As a result, the foil surfaces were frequently found to be rough and scratched on a micron scale. Fortunately, this only complicates, but does not prevent, the identification of impact craters.

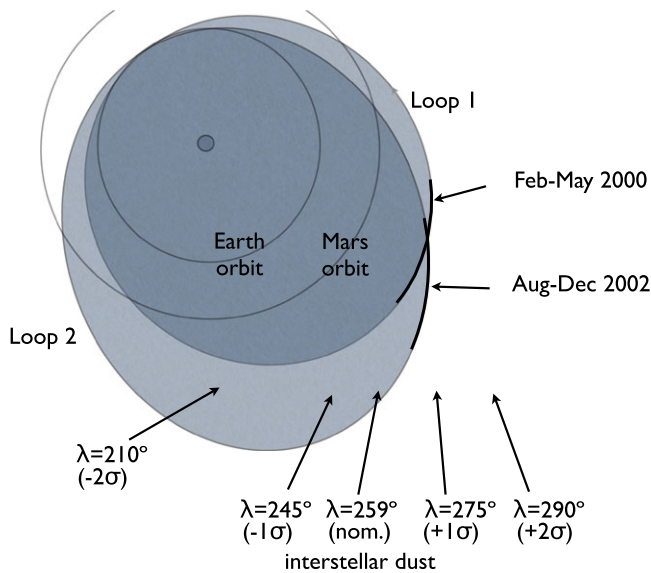


Fig. 1. Schematic diagram of exposures (thick portion of orbits) of the Stardust interstellar collector to the interstellar dust stream. The interstellar dust stream is coincident with the ecliptic within errors. We indicate the nominal radiant longitude,  $259^\circ$ , along with values  $\pm 1\sigma$  and  $\pm 2\sigma$  different from the nominal value. Figure adopted from JPL Stardust mission plan ([http://pdssbn.astro.umd.edu/holdings/sdu-a-navcam-2-edr-annefrank-v1.0/document/mission\\_plan.pdf](http://pdssbn.astro.umd.edu/holdings/sdu-a-navcam-2-edr-annefrank-v1.0/document/mission_plan.pdf)).

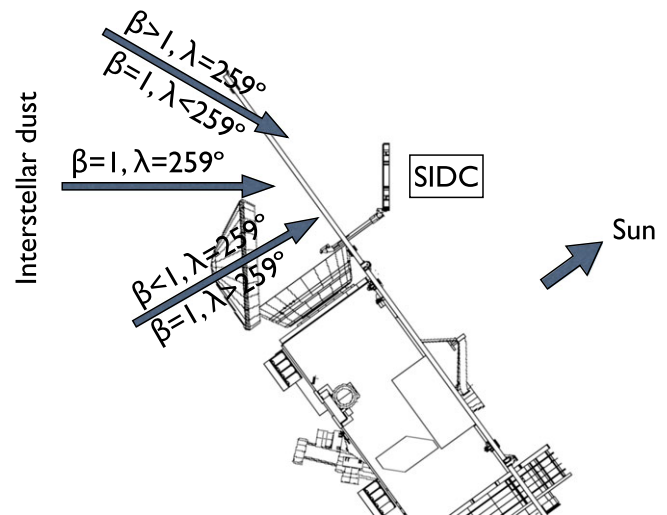


Fig. 3. Orientation of the spacecraft and interstellar dust collector near the beginning of each exposure. The collector was oriented so that particles from the nominal interstellar radiant with  $\beta = 1$  would be collected at normal incidence to the collector. Particles with  $\beta < 1$  or with a radiant longitude greater than nominal value would be collected with a sunward (“midnight”) trajectory, and particles with  $\beta > 1$  or with a radiant longitude less than nominal value would be collected with an antisunward (“6 o’clock”) trajectory. Figure adopted from JPL Stardust mission plan ([http://pdssbn.astro.umd.edu/holdings/sdu-a-navcam-2-edr-annefrank-v1.0/document/mission\\_plan.pdf](http://pdssbn.astro.umd.edu/holdings/sdu-a-navcam-2-edr-annefrank-v1.0/document/mission_plan.pdf)).

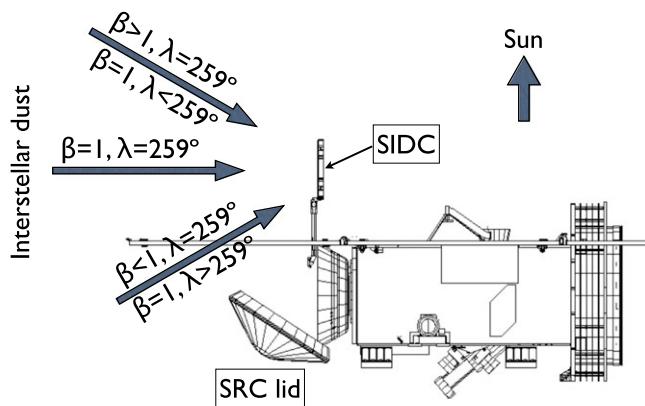


Fig. 2. Typical orientation of the spacecraft and interstellar dust collector during exposures to the interstellar dust stream. The collector was oriented so that particles from the nominal interstellar radiant with  $\beta = 1$  would be collected at normal incidence to the collector. However, particles with  $\beta < 1$  or with a radiant longitude greater than nominal value would be collected with a sunward (“midnight”) trajectory, and particles with  $\beta > 1$  or with a radiant longitude less than nominal value would be collected with an antisunward (“6 o’clock”) trajectory. Figure adopted from JPL Stardust mission plan ([http://pdssbn.astro.umd.edu/holdings/sdu-a-navcam-2-edr-annefrank-v1.0/document/mission\\_plan.pdf](http://pdssbn.astro.umd.edu/holdings/sdu-a-navcam-2-edr-annefrank-v1.0/document/mission_plan.pdf)).

### ISPE: LOGISTICS, METHODS, AND CONSTRAINTS

The Stardust Interstellar Preliminary Examination is the fourth NASA Preliminary Examination (PE) of returned extraterrestrial samples, after the Apollo PE, the Long Duration Exposure Facility PE, and the Stardust Cometary PE. As with previous PEs, NASA supported the ISPE to provide basic characterization of the returned sample, to support curation of the sample into the indefinite future, to inform sample requests from future investigators, and to provide adequate information to allow the allocation subcommittee to evaluate sample requests. The goals of the ISPE were deliberately limited to answering the following questions:

1. How many tracks in the collector are consistent in their morphology and trajectory with interstellar particles?
2. How many of these potential tracks are consistent with real interstellar particles, based on chemical analysis? Conversely, what fraction of candidates are consistent with either a secondary or interplanetary origin?
3. What is the mass distribution of these particles, and what is their state? Are they particulate or diffuse? Is there any crystalline material?

4. How many detectable impact craters (>100 nm) are there in the foils, and what is their size distribution?
5. How many of these craters have analyzable residue that is consistent with extraterrestrial material? Can craters from secondaries be recognized through crater morphology (e.g., ellipticity)?

The ISPE did not seek to answer the following questions regarding dust from the local interstellar medium:

1. What is its isotopic composition?
2. What is its mineralogy/petrology?
3. What are its trace elemental abundances?

To answer the first five questions above, we proposed to the Curation and Planning Team for Extraterrestrial Materials (CAPTEM) in 2007 to carry out nondestructive, noninvasive analyses of interstellar dust candidates. For particles trapped in aerogel, we employed synchrotron-based X-ray and infrared microprobes, at high spatial resolution, of interstellar dust candidates extracted from the aerogel collectors in picrokeystones. For particles captured as residues in craters in aluminum foil, we identified and analyzed craters using FE-SEM and Auger analysis. The following techniques were specifically excluded from the ISPE:

1. Analyses requiring techniques that have not been demonstrated on picogram samples in aerogel or on picogram residues in foils.
2. Any technique that requires invasive or destructive sample preparation (e.g., dissection, wafering, ultramicrotomy) or is itself destructive (e.g., SIMS). Invasive and destructive sample preparation and analyses (e.g., TEM, SIMS, L<sup>2</sup>MS) would be performed only on samples released from ISPE, with the exception of TEM work on impact craters.

We organized the ISPE in six parallel efforts:

1. Identification of impacts in aerogel using automated digital microscopy and a distributed, internet-based search by volunteers (Westphal et al. 2014)
2. Extraction of tracks in “picrokeystones” and photodocumentation (Frank et al. 2013)
3. Characterization of impacts by synchrotron infrared and X-ray microprobes (Bechtel et al. 2014; Brenker et al. 2014; Butterworth et al. 2014; Flynn et al. 2014; Gainsforth et al. 2014; Simionovici et al. 2014)
4. Search for, and nondestructive analysis of, impacts in the Stardust interstellar collector aluminum foils (Stroud et al. 2014)
5. Laboratory simulations of interstellar dust captured in aerogel using the Heidelberg dust accelerator (Postberg et al. 2014)
6. Numerical modeling of propagation and kinetics of interstellar dust particles in the heliosphere (Sterken et al. 2014)

In this volume of MAPS, we present the final suite of reports from the Interstellar Preliminary Examination (ISPE):

Westphal et al. (ISPE I) report on the identification of 71 unambiguous tracks in the Stardust Interstellar Collector, principally identified by amateur scientists through an internet-based search of digital optical micrographs called Stardust@home.

Frank et al. (ISPE II) describe the extraction of tracks and other possible impact features in “picrokeystones,” and subsequent optical photodocumentation, and make recommendations for future curation of interstellar candidates. They also discuss backgrounds, both from secondary ejecta of material from impacts on the spacecraft, and also from Interplanetary Dust Particles.

Bechtel et al. (ISPE III) report on the search for organic materials in interstellar candidate tracks using synchrotron-based Fourier transform infrared microscopy.

Butterworth et al. (ISPE IV) report on the analyses of major rock-forming elements in interstellar candidates using synchrotron-based scanning transmission X-ray microscopy (STXM), the only technique that can perform such analyses of particles while still embedded in aerogel.

Brenker et al. (ISPE V) report on the analysis of heavy elements in several interstellar candidates using synchrotron X-ray fluorescence (SXRF) beamline ID13 at the European Synchrotron Radiation Facility (ESRF).

Simionovici et al. (ISPE VI) report on the analysis of heavy elements in several interstellar candidates using the SXRF beamline ID22 at ESRF.

Flynn et al. (ISPE VII) report on the analysis of heavy elements in several interstellar candidates using the SXRF beamline 2-ID-D at the Advanced Photon Source.

Gainsforth et al. (ISPE VIII) report on the analysis of X-ray diffraction (XRD) data collected at ID13 and ID22 on two interstellar candidates.

Postberg et al. (ISPE IX) report on the results of laboratory simulations of interstellar dust impacts into Stardust flight-spare aerogel tiles. These results enabled us to constrain the impact speed of interstellar candidates.

Sterken et al. (ISPE X) report the results of numerical modeling of the propagation of interstellar dust in the heliosphere, giving the distribution of impact speeds and trajectories.

Stroud et al. (ISPE XI) report on the identification of impact craters in the aluminum foils of the Stardust Interstellar Collector, along with analyses of residues in the several craters.

## ASTROPHYSICAL CONTEXT

The goal of the Interstellar Dust Collection component of the Stardust mission was to collect and return the first solid samples of material from beyond the solar system. It is important to emphasize that this collection is local—that is, from the circumheliospheric interstellar medium (CHISM)—and that the findings from analyses of these samples cannot be generalized in a straightforward way to the “average” interstellar medium (ISM). Indeed, it is not clear that the concept of an average ISM is useful: although the ISM is thought to be chemically well mixed through MHD turbulence (Draine 2009), the ISM comprises environments—from hot, low-density bubbles to cold molecular clouds—that exhibit extreme contrasts in temperature and density that far exceed those, for example, among the familiar solids, liquids, and gasses in our terrestrial surroundings. This is reflected in large variations in abundances in the gas phase, which, assuming a universal composition of the combined phases, implies large variations in dust composition (Frisch and Slavin 2013).

Frisch et al. (2012) have recently reviewed the state of knowledge of our local interstellar neighborhood, and presented a picture of the local interstellar environment based on absorption measurements to nearby stars as well as observations of neutral interstellar gas in the solar system. In their picture, the Sun is located within a cluster of approximately 15 moderate-density, warm clouds, all located within approximately 10 pc, called the cluster of local interstellar clouds (CLIC). We are located in or near the edge of a low-density, partially ionized cloud called the local interstellar cloud (LIC), and are close to a similar, neighboring cloud, the “G” cloud. Measurements on interstellar neutral He flowing into the heliosphere enable the determination of some physical parameters of the CHISM, given in table 2 of Frisch et al. (2012). Some key parameters of the CHISM are temperature— $6680 \pm 1490$  K, density—approximately  $0.2 \text{ cm}^{-3}$ , diameter approximately 2.5 pc, and turbulent velocity  $2.2 \pm 1.0 \text{ km s}^{-1}$ . The CLIC is located in the interior of the local bubble (LB), a hot, nearly evacuated bubble approximately 200 pc in size, with a temperature approximately 100 times higher and a density approximately 100 times lower than the LIC. Tiny, cold molecular clouds are also present in the neighborhood of the CLIC, such as the nearby local Leo cold cloud (Meyer et al. 2012), which have temperatures  $>100$  times lower and densities  $>10^4$  times higher than those in the warm CLIC clouds. Such clouds could plausibly be the source of large ( $>1 \mu\text{m}$ ) interstellar grains (Frisch and Slavin 2013).

The size scale of gradients in the ISM is sufficiently small that CHISM conditions may vary on the time

scale of approximately  $10^4$  yr (Frisch and Slavin 2006). Indeed, we are fortunate to live in an epoch in which interstellar dust is present in the CHISM—before the late Quaternary, the solar system was probably located in the nearly empty LB, and little or no interstellar dust would have been available for collection (Frisch and Slavin 2006).

There are fundamental selection effects that complicate the interpretation of the collection. In enumerating these selection effects, we work from the edge of the heliosphere inward. Propagation of dust crossing into the heliosphere and propagation of dust within the heliosphere are determined by the interaction with quasi-static electromagnetic fields, and by the repulsive pressure exerted by sunlight. In principle, these are completely determined for any given particle by its magnetic rigidity  $R$ , and by  $\beta$ , which is the dimensionless ratio of the radiation force due to sunlight to the solar gravitational force. However, this is complicated in practice because an accurate calculation assumes perfect knowledge of the configuration of the complicated interplanetary magnetic fields, and also a knowledge of the history of  $\beta$ , which may be changing, for example, due to evaporation of ices. Because of their small magnetic rigidities, very small (approximately 10 nm) interstellar dust particles do not penetrate the heliopause (Slavin et al. 2009). Intermediate-sized (approximately 100 nm) grains are subject to Lorentz forces and the outward propagation of the solar wind. The propagation of large (approximately  $1 \mu\text{m}$ ) particles is determined mostly by solar light pressure forces, and is determined by  $\beta$ . As described by Sterken et al. (2014) in this issue, particles with  $\beta > 1.6\text{--}1.8$  do not penetrate to the position of the Stardust spacecraft.

After capture, identification of tracks is a major challenge. As described by Sterken et al. (2014), the capture speed of particles in the Stardust collector depends strongly on  $\beta$ : capture speeds as low as approximately  $2 \text{ km s}^{-1}$  are possible for particles with high  $\beta$ , while particles with  $\beta \sim 0$  are captured at  $>20 \text{ km s}^{-1}$ . In turn, the detection efficiency of particles depends principally on the track diameter, as described by Westphal et al. (2014), and while the detection efficiency is high for  $>2.5 \mu\text{m}$  diameter tracks, below this size the detection efficiency is not well constrained. The track diameter, in turn, is a function of both particle speed and size; laboratory experiments that constrain this function are reported in this volume by Postberg et al. (2014). The collection is therefore biased toward larger particles at a given capture speed, but biased toward faster particles for a given particle size. However, as illustrated by Track 40 (Sorok (Butterworth et al. 2014), particles survive capture well only at lower speeds.

Data from dust detectors onboard the Galileo and Ulysses spacecraft have indicated the presence of a stream of interstellar dust in the heliosphere (Grün et al. 1993). This dust stream has unanticipated properties. Perhaps the most perplexing is the unexpectedly large flux of large interstellar dust grains, which appears to violate astronomical constraints on the mass density and distribution of dust in the LIC (see Draine [2009], for a recent discussion). Based on these observations, Landgraf et al. (2006) estimated that the Stardust Interstellar Collector would collect approximately 40 particles greater than roughly 1  $\mu\text{m}$  in radius, and approximately 80 particles less than 1  $\mu\text{m}$  in radius. These estimates were made after the Stardust launch, but before the actual exposures were carried out. This estimate assumed a collection time of 290 days, while the actual collection time was 195 days. After the successful Wild2 encounter, there was a strong desire to protect the captured cometary samples and not to reopen the sample collector again, so the science team decided to forgo the third interstellar sample collection (Tsou et al. 2003). With the simplifying assumption that the flux is constant over the collection periods, a corrected estimate gave approximately 25 particles greater than 1  $\mu\text{m}$  in radius, and approximately 50 particles less than 1  $\mu\text{m}$  in radius to have impacted the collector.

Remote and in situ observations give little guidance that would allow us to decide whether or not any particular particle has an interstellar origin, for several reasons. First, while astronomical observations of interstellar dust and of interstellar gas give valuable information about the bulk properties of interstellar dust, the diversity of individual particles is essentially unconstrained. Second, it is not known whether or not the largest particles are representative of the average dust population. Most of the mass of interstellar dust is thought to reside in grains with masses less than 500 fg (Draine 2009). The overabundance of large particles as observed by Ulysses and Galileo (Grün et al. 1995; Krüger et al. 2006), if combined with the astronomically derived size distribution of small grains, violates constraints on cosmic abundances (Frisch et al. 1999; Draine 2009). Whether or not this is a fundamental problem with one of the observations, or if the CHISM is locally enriched in large grains, perhaps originating from a local cold molecular cloud such as the Leo cloud (Frisch and Slavin 2013), is not yet known. The observation in Ulysses data of a size-independent, 30° shift in the direction of the interstellar dust stream around 2006 may imply inhomogeneities in the local dust environment on a surprisingly small scale (Draine 2009; Krüger et al. 2010).

## LIMITATIONS OF THE ISPE AND IDENTIFICATION OF INTERSTELLAR PARTICLES

Adding to the technical challenge of working with these samples were the limitations imposed by the ISPE rules. It was recognized from the beginning of the ISPE that definitive identification of interstellar dust might not be forthcoming during the ISPE. This is principally due to lack of compositional signatures, experimentally accessible during the ISPE, that would decisively distinguish between interstellar and interplanetary dust. A detection of an interstellar component among tracks in the aerogel might have to rely on a statistical excess of trajectories pointing back into the direction of the interstellar dust stream, against a background of interplanetary dust impacts with a different distribution of trajectories.

An aspect that was not anticipated at the beginning of the ISPE was that impact velocity can give additional constraints. Although particles with  $\beta \sim 0$  impact the collector at high speeds ( $\gg 10 \text{ km s}^{-1}$ ), particles with  $\beta > 1$  can impact at low speed, as low as  $2 \text{ km s}^{-1}$ . Because impact speed is well correlated with  $\beta$ , constraints on impact speed by comparison of track morphology with calibrations from laboratory analog experiments can constrain  $\beta$ . This, in turn, can constrain the structure of interstellar dust: large  $\beta$  can be indicative of a fluffy, fractal-like structure, while small  $\beta$  is expected for compact, quasi-spherical particles.

Some bulk properties of interstellar dust are known through infrared and X-ray observations of the ISM. However, the properties of individual interstellar dust particles are largely unconstrained. It was understood from the beginning of the ISPE that the identification of interstellar dust particles in the Stardust Interstellar Dust Collector therefore is a process of elimination of other possibilities.

## ANSWERS TO ISPE QUESTIONS

Here, we report the answers to the questions that we set out to answer during the ISPE.

### How Many Tracks Are Consistent in Their Morphology and Trajectory with Interstellar Particles?

As described above, this question turned out to be unexpectedly complex. Once identified, determination of track trajectory with respect to the collector is straightforward. However, the question of consistency of trajectory with an interstellar origin is complicated by three effects: tray articulation during exposures, spacecraft stabilization, and uncertainties in the interstellar dust model.

First, as discussed in the companion papers by Sterken et al. (2014) and Frank et al. (2013), the tray was articulated with respect to the spacecraft during the two exposures to the interstellar dust stream, to approximately track the radiant for particles with  $\beta = 1$ , with an assumption that the interstellar radiant was located at ecliptic coordinates  $+8^\circ$  latitude,  $259^\circ$  longitude. Although the articulation of tray as a function of time is well understood, the timing of each impact is of course unknown. Furthermore, it so happened that, because of the particular configuration of the spacecraft with respect to the interstellar radiant direction during the exposures, the trajectories of particles in the frame of the spacecraft were very sensitive to uncertainties in the radiant longitude. Second, the spacecraft was maintained in a deadband of  $\pm 15^\circ$  in roll, pitch, and yaw around the position defined by the interstellar radiant and the Sun-spacecraft vector. Finally, and most importantly, there are significant uncertainties in the radiant position (Frisch et al. 1999). The largest uncertainty is in the radiant longitude, and while the  $1\sigma$  uncertainty encompasses  $245^\circ \leq \lambda \leq 275^\circ$ , the  $2\sigma$  uncertainty is considerably wider, and encompasses  $210^\circ \leq \lambda \leq 290^\circ$  (Frisch et al. 1999). In Fig. 4, we show the results of a Monte Carlo simulation in which we made the following assumptions:

1. For each trial, the radiant longitude was picked from a Gaussian distribution centered on  $\lambda = 259^\circ$  with a width of  $20^\circ$ .
2. The radiant latitude was fixed at  $+8^\circ$ .
3.  $\beta$  was drawn from a flat distribution between 0 and 1.6 (the cutoff at the Stardust spacecraft).
4. Impact times were evenly distributed across both exposure periods.
5. The velocity of the dust at infinity is  $26 \text{ km s}^{-1}$ , and has zero dispersion.

Of the 71 unambiguous tracks that have been identified, 25 tracks ( $35 \pm 7\%$ ) had an azimuth within approximately  $20^\circ$  of the sunward direction in the frame of the spacecraft. As shown in fig. 2 of Frank et al. (2013) none were found with a direction pointing antisunward, corresponding to the points below the origin in Fig. 4. The remaining 46 tracks have a direction that is approximately consistent with an origin as secondaries from impacts on the aft solar panels. We have only analyzed four of these, on the assumption that this is the most likely origin for most of these tracks, as the solar panels also would have blocked interstellar dust particles from that direction. We confirmed an origin from the Cerich glass covers of the solar panels, but point out that it is possible that some of these particles have an interplanetary or interstellar origin, based on Fig. 4.

We have now searched approximately half of the Stardust Interstellar tray, and have analyzed

approximately half of the tracks whose trajectories are consistent with an interstellar origin. We have referred to this population as the so-called “midnight tracks” because of their orientation on the face of a clock (Fig. 4). In principle, this could also include tracks in the 6 o’clock direction on the clock, but we not yet identified any tracks with this orientation. Assuming that interstellar dust particles will be found only among the midnight population, we estimate that the entire interstellar dust collection in aerogel consists of approximately 12 particles. That the collection is substantially smaller than anticipated is not yet understood, but it is unlikely to be due to identification inefficiency, as we describe in Westphal et al. (2012).

### **How Many of These Potential Tracks Are Consistent with Real Interstellar Particles, Based on Chemical Analysis? Conversely, What Fraction of Candidates Are Consistent with Either a Secondary or Interplanetary Origin?**

As described in companion papers by Brenker et al. (2014), Butterworth et al. (2014), Flynn et al. (2014), and Simionovici et al. (2014), of the 12 “midnight” tracks for which we have definitive analyses, eight were identified as definite or probable secondary ejecta from the spacecraft deck, and three have properties that are inconsistent with an origin as secondaries. On the assumption that all of the nonmidnight tracks have a secondary origin, and that all three of tracks 30, 34, and 40 are interstellar, we find that  $4_{-2}^{+4}\%$  of all of the tracks, and  $27_{-14}^{+20}\%$  of the midnight tracks, have an interstellar origin. (See Gehrels [1986] for the derivation of the  $1\sigma$  confidence intervals.)

The interplanetary dust fluence in the Stardust Interstellar Dust Collector (SIDC) is discussed by Frank et al. (2013). The absence of tracks in a significant fraction of possible azimuths implies that the interplanetary dust fluence as a background for interstellar dust is not large, but more work is necessary to characterize it. Nevertheless, the flux of interplanetary dust appears to be consistent so far with estimates from models (Altobelli, personal communication).

Because no single characteristic is an unambiguous indicator of interstellar origin, we define levels of candidacy for interstellar origin.

#### ***Aerogel Collectors***

Level 0: A track or other impact-like feature in aerogel.

Level 1: A definite track or impact confirmed by high-resolution optical microscopy.

Level 2: A trajectory consistent with interstellar origin and composition inconsistent with spacecraft materials.

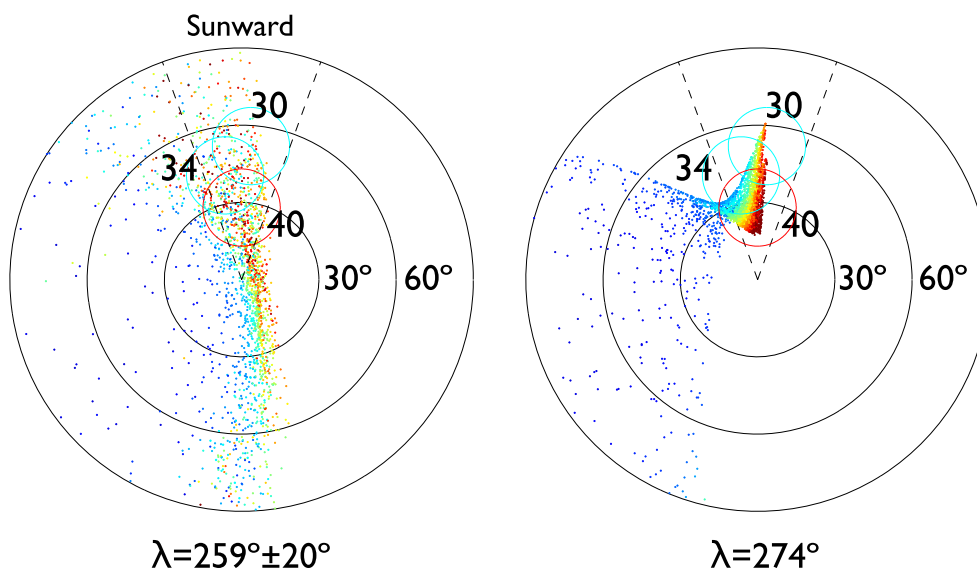


Fig. 4. (Left) Plot of calculated trajectories of particles in Monte Carlo simulations, consistent with the uncertainties in the interstellar dust propagation model, as recorded in the Stardust Interstellar Dust Collector. On this polar plot, track zenith angles correspond to the radial dimension, and the azimuth is the angular dimension; particles at normal incidence plot at the center, sunward-directed particles above the center, and antisunward particles below the center. The color coding indicates capture speed, from dark blue ( $1.9 \text{ km s}^{-1}$ ) to bright red ( $\geq 25 \text{ km s}^{-1}$ ). Only a subset of this distribution, one that would correspond to the actual value of the interstellar radiant, would actually be observed, but a comparison of this distribution with measurements of actual candidates addressed the question of consistency between interstellar dust candidates and what is known about the interstellar dust radiant. The dashed lines bound the approximate region in which secondary ejecta from impacts on the deck of the sample return capsule (SRC) would be found. The large circles are the approximate confidence intervals of the three interstellar candidates that appear to be consistent with an origin in the interstellar dust stream, two (30 and 34) are not consistent in composition with SRC materials, and the third (40) has a capture speed inconsistent with secondary ejecta. The colors of the candidate confidence intervals reflect estimates of capture speed. (Right) The same figure, but with a specific choice of radiant longitude ( $274^\circ$ ) that is consistent with the hypothesis that tracks 30, 34, and 40 are interstellar.

Level 3: O isotopic composition inconsistent with solar values.

#### Aluminum Foils

Level 0: An impact-like feature in aluminum foil.

Level 1: A definite crater confirmed by SEM.

Level 2: Composition inconsistent with spacecraft materials.

Level 3: O isotopic composition inconsistent with solar values.

In Table 1, we present a summary of the features extracted and analyzed during the ISPE. Table 2 is a summary of tracks identified, but not extracted, and therefore not yet analyzed, during the ISPE. Table 3 is a summary of candidate impacts in foils that were analyzed during the ISPE.

#### What Is the Mass Distribution of These Particles, and What Is Their State? Are They Particulate or Diffuse? Is There Any Crystalline Material?

In two cases, we were able to measure masses because the terminal particles were completely intact,

with no detectable residue in the upstream tracks. We estimated the mass of the terminal particle of track 30, Orion, to be  $3.0 \pm 0.3 \text{ pg}$ , and that of the terminal particle of track 34, Hylabrook, to be approximately  $4.4 \text{ pg}$ . With reasonable assumptions about the hidden dimension (parallel to the analytical beams) of the particles, we found their densities to be approximately  $0.7 \text{ g cm}^{-3}$  and  $0.34 \text{ g cm}^{-3}$ , respectively. The morphology of the tracks, the lack of track residues upstream of the terminal particles, and the compact nature of the terminal particles themselves all point to low capture speeds, probably  $< 10 \text{ km s}^{-1}$ . Track 40, by contrast, contains no convincing residues of the original projectile, almost certainly because of a large capture speed. The projectile residues are likely to be diffuse and trapped in walls of the track. Using a model derived from the Heidelberg calibration experiments (Postberg et al. 2014), we estimate the mass of the track 40 projectile to be approximately  $3 \text{ pg}$ , assuming a capture speed of  $15 \text{ km s}^{-1}$ .

Synchrotron X-ray absorption near-edge spectra (XANES) (Butterworth et al. 2014) and XRD topographs (Gainsforth et al. 2014) of tracks 30 and 34 indicate that



Table 1. List of samples extracted from aerogel tiles and analyzed during the Stardust Interstellar Preliminary Examination.

JSC ID	Stardust@home ID	Alias	Analysis	Refs.	Interpretation
I1017,2,1	6355541V1		Mg, Al, K, Ti, Fe, Zn, Ce	3,4,5	SP secondary
I1004,1,2	862370V1		Amorphous Al oxide	4,7	ISC level 1
I1004,2,3	730481V1		Mg, Al, Ce, Zn	4,6	SP secondary
I1007,1,4	5088094V1		Na, Mg, Al, Zn, Ce	3,4	SP secondary
I1006,1,5	8130472V1		Ce, Mg, Al, minor Na	3,4,6	SP secondary
I1029,1,6	Many, e.g., 421890V1		Corundum, amorphous Mg, Na, Al	3,4	Secondary of unknown origin
I1027,1,9	9471219V1		Cl, Ti, Fe, Cu, Zn	3,6	Contaminant
I1029,4,10	Many, e.g., 421890V1		Weak Na, Al; No Ce, Mg, Fe	3,4	Secondary of unknown origin
I1032,1,11	4589365V1		Alumina	3,4	Contaminant
I1093,1,12	5637295V1		Cr, Cu, Br	3,6	Contaminant
I1081,1,13	404198V1		Cu, Zn, Se, Br	3,6	Contaminant
I1059,1,14	3602277V1		Cu, Zn, Se, Br	3,6	Contaminant
I1029,5,15	9267050V1		Cu, Zn, Se, Br	3,6	Contaminant
I1001,1,16	598677V1		Fe, Zn	3,7	Contaminant
I1001,2,17	4823551V1		Cr, Fe, Ni, Zn	3,7	Surface contaminant?
I1013,2,19	1516035V1		Si, Mg, Al	3,4	Not an impact
I1017,6,20	8446209V1		Cr,Mn,Fe,Ni	3,4,5	Not an impact
I1004,3,21	4020226V1		Si	3,4,5	Not an impact
I1031,1,23	421890V1		Si, minor Na, Al	3,4	Not an impact
I1006,3,24	772902V1		Si, minor Al, Fe, Ni, Zn	3,4	Not an impact
I1075,1,25	363295V1		K, Ti, V, Cr, Mn, Fe, Cu, Zn	4,7	Contamination
I1093,2,26	Many, e.g., 9688223V1		None detected	4	Artefact of tile insertion
I1093,3,27			Zn	7	Surface contaminant
I1060,1,28	3914098V1		Metallic and oxidized Al	4,5	SRC secondary from Al-mylar foil
I1059,2,29	8894764V1		Al metal	4,5	SRC secondary
<b>I1043,1,30</b>	<b>7663035V1</b>	<b>Track 30, Orion</b>	<b>Spinel, olivine, amorphous Mg-, Al-bearing phase, Fe-bearing phase</b>	<b>4,5,6,8</b>	<b>ISC level 2</b>
I1059,3,31	5356462V1		Mg, metallic, oxidized Al	4	Contamination
I1044,2,32	2604819V1		Ni, Fe	4,7	ISC level 0
I1044,3,33	7068V1		None detected <sup>a</sup>	4,7	Possible IDP
<b>I1047,1,34</b>	<b>1203103V1</b>	<b>Track 34, Hylabrook</b>	<b>Mg-rich Olivine, Fe, Si, Al</b>	<b>4,5,8</b>	<b>ISC level 2</b>
I1032,2,35	2205922V1		Al metal, Al oxide	4	SRC secondary
I1032,3,36			Al metal, amorphous Al oxide	4	SRC secondary
I1092,1,37	3160814V1	Track 37, Merlin	Amorphous Al oxide, C, minor Fe, F	3,4,5	SRC secondary
I1092,2,38	4359211V1		Too dense for STXM	4	ISC level 1
I1017,1,39	5599106V1		Al metal	4	SRC secondary
<b>I1003,1,40</b>		<b>Track 40, Sorok</b>	<b>Possible C, Fe; no terminal particle</b>	<b>3,4</b>	<b>ISC level 2</b>
I1097,1,41	5848045V1		Al metal	4	SRC secondary
I1048,1,42	5484077V1		Al metal	4	SRC secondary

SP = solar panel; SRC = sample return capsule; ISC = interstellar candidate. ISC levels are defined in the text. Level 2 candidates are indicated in bold.

<sup>a</sup>Small possible impact feature with Ca, Ti, Cr, Mn, Ni, and Cu to Fe ratios near CI, but elevated K and Zn, and depleted S, 40  $\mu\text{m}$  away. Source: 3: Bechtel et al. (2014), 4: Butterworth et al. (2014), 5: Brenker et al. (2014), 6: Simionovici et al. (2014), 7: Flynn et al. (2014), 8: Gainsforth et al. (2014).

both contain crystalline olivine, and track 30 contains crystalline fraction in either case, but in both cases, we spinel. We were not able to accurately measure the found that the crystalline fraction is substantial (>10%).

Table 2. List of unambiguous tracks identified in aerogel tiles, but not extracted or analyzed during the Stardust Interstellar Preliminary Examination.

Stardust@home ID	Interpretation
225116V1	SP secondary
237326V1	SP secondary
2574341V1	SP secondary
433711V1	SP secondary
451142V1	SP secondary
1303955V1	ISC level 1
1728279V1	SP secondary
3059039V1	SP secondary
7387315V1	SP secondary
3997562V1	SP secondary
9987464V1	SP secondary
1779983V1	SP secondary
6389213V1	SP secondary
6721021V1	SP secondary
6842109V1	SP secondary
7559378V1	SP secondary
7933874V1	SP secondary
5103315V1	SP secondary
1078907V1	SP secondary
2344842V1	SP secondary
4969429V1	SP secondary
6366986V1	SP secondary
6474626V1	ISC level 1
6522857V1	SP secondary
6535376V1	SP secondary
1218276V1	SP secondary
5300933V1	SP secondary
2599361V1	ISC level 1
8250577V1	SP secondary
5198758V1	SP secondary
9219038V1	SP secondary
661377V1	ISC level 1
1506030V1	ISC level 1
2923270V1	SP secondary
4563629V1	ISC level 1
6279005V1	SP secondary
8454485V1	SP secondary
8806280V1	SP secondary
31269V1	SP secondary
9732478V1	SP secondary
2715058V1	ISC level 1
6493751V1	SP secondary
19284V1	ISC level 1
709134V1	ISC level 1
2293539V1	SP secondary
3726006V1	SP secondary
4028216V1	ISC level 1
6031444V1	ISC level 1
7510686V1	SP secondary
9751354V1	SP secondary
9659008V1	SP secondary

Table 2. *Continued.* List of unambiguous tracks identified in aerogel tiles, but not extracted or analyzed during the Stardust Interstellar Preliminary Examination.

Stardust@home ID	Interpretation
5958593V1	SP secondary
6125350V1	SP secondary
535699V1	SP secondary

### How Many Detectable Impact Craters (>100 nm) Are There in the Foils, and What Is Their Size Distribution?

Stroud et al. (2014) report the discovery of 25 confirmed impacts in 4.84 cm<sup>2</sup> of Stardust Interstellar aluminum foils, which corresponds to an average density of  $5.1 \pm 1.0$  cm<sup>-2</sup>. In practice, due to the surface quality of the foils and practical limitations of scanning, the actual detection threshold in crater diameter was close to 200 nm.

### How Many of These Craters Have Analyzable Residue that Is Consistent with Extraterrestrial Material? Can Craters from Secondaries Be Recognized through Crater Morphology (e.g., Ellipticity)?

Stroud et al. (2014) report the discovery of four craters with residues consistent with extraterrestrial material.

## CHALLENGES AND OUTSTANDING QUESTIONS

In many ways, the ongoing analysis of the Stardust Interstellar Collection presents unprecedented challenges. Some were anticipated and some were unanticipated at the beginning of the ISPE.

1. The particles are approximately 1 pg in mass,  $<10^{-3}$  of the mass of particles in the other small-particle collections that NASA curates (Stardust cometary samples and cosmic dust).
2. The total number of interstellar particles near 1  $\mu$ m in size is probably of order 10.
3. The fluence of impacts in the collector is extremely small, of order one interstellar candidate per 100,000 fields of view in search optical photomicrographs.
4. Unlike the Stardust cometary collection, the “signal-to-noise” is small: for each track containing extraterrestrial material, there are approximately 25 tracks due to secondary ejecta from impacts on the spacecraft.

Table 3. Summary of crater candidate analyses. In addition to the listed elements, Al, C, and O were detected for all craters. Elements listed in italics are tentative detections. Details of the analyses are presented in Stroud et al. (2014). Level 2 candidates are shown in bold.

Crater search	JSC ID	Elements detected	Candidate level
1) 1031N,1 37@02		B,Mg,Si,Ti,Ce	Solar cell secondary
<b>2) 1044N,1 12a_0277</b>	<b>I1044N,3</b>	<b>Mg,Si,S,Fe</b>	<b>2</b>
3) 1061N,1 41@33		F,Mg,Si	Solar cell secondary
4) 1092W,1 4_3		Mg,Si,Ti,Fe Ce	Solar cell secondary
5) 1061N,1 22@44		Mg,Si	1
6) 1033N,1 5_71		n.d.	Plucked impurity or SRC sec.?
<b>7) 1061N,1 36@33</b>	<b>I1061N,3</b>	<b>Mg,Si,S,Fe,Ca,Cr</b>	<b>2</b>
<b>8) 1061N,1 69@22</b>	<b>I1061N,4</b>	<b>Mg,Si,S,Fe,Ni</b>	<b>2</b>
9) 1044N,1 34_0317		Si, Ce, Zn,Na	Solar cell secondary
10) 1092W,1 5_29		Si,Na,Ti,Zn,Ce	Solar cell secondary
<b>11) 1061N,1 135@30</b>	<b>I1061N,5</b>	<b>Mg,Si,S,Fe,Ni,Ca,Cr</b>	<b>2</b>
12) 1010W,1 12_7		n.d.	Plucked impurity
13) 1031N,1 158@35		B,F,Mg,Si,Ti,Ce	Solar cell secondary
14) 1044N,1 06e_0143		Si,Fe	Foil impurity + sec.
15) 1031N,1 239@11		Mg,Si	1
16) 1061N,1 205@32		B,Si,Ce,Mg	Solar cell secondary
17) 1031 216@45		Mg,Si	1
18) 1061 188@24		Si, B	Solar cell secondary
19) 1019W,1 01e_0002		F,Mg,Si,Na,Zn,Ce	Solar cell secondary
20) 1044N,1, 06e_251		Si,Fe,Ni	Foil impurity + sec.
21) 1033N,1 11_175		Mg,Si,K,Ti,Fe,Zn,Ce	Solar cell secondary
22) 1077W,1 499		Fe	Foil impurity
23) 1047N,1 177@14		Fe	Foil impurity
24) 1077W,1 387		Mg,Si,K,Fe,Ti,Zn,Ce	Solar cell secondary
25) 1018N,1		Pending	Foil impurity

5. Distinguishing signal from background requires synchrotron-based X-ray microprobes, which are typically heavily oversubscribed.

We observed modification of the terminal particles of two tracks during the course of the ISPE analyses, reported by Butterworth et al. (2014) and Simionovici et al. (2014). In one case, track 30, the change was very significant, with the loss of most of the Fe and Ni from the particle, and into the track and surrounding aerogel, and the physical separation of two components of the terminal particle. After an investigation, we eliminated synchrotron X-ray analyses as the immediate cause of these changes, and concluded that they were likely to have occurred between, not during, synchrotron analyses. Whether this was a result of “weathering” in the terrestrial oxygen-rich atmosphere, or had some other cause, is not yet understood. We also observed the relatively minor physical disruption of track 34 and one of the particles in track 30 during subsequent analyses. These effects are now understood to have been due to exceeding the self-imposed fluence limits on these particles by approximately two orders of magnitude. Based on the observation that particles did not detectably change in mass, morphology, or chemistry under normal

conditions during synchrotron analyses, we conclude that soft X-ray and hard X-ray synchrotron microprobes are safe for future analyses, if fluence limits, described in Brenker et al. (2014) and Butterworth et al. (2014) are respected. However, we add the caveat that, until the initial modification of track 30 is completely understood, there remains the possibility that synchrotron analysis was directly or indirectly associated with this event, either through an undocumented, anomalous, and probably rare, overexposure, or perhaps through enhanced chemical reactivity of the particle induced by the X-ray analysis. Ongoing and future experiments with analogs may answer this question. We also found that hard X-ray synchrotron analyses resulted in detectable contamination by organics, while soft X-ray (STXM) analyses did not.

Post-ISPE analyses, which may be allowed, in principle, to be destructive, may be decisive in determining interstellar origin. Probably the highest priority, both for particles in aerogel and residues in foil craters, will be measurement of O isotopes, to confirm origin in the local ISM. It is known from astronomical observations that the solar system is strongly anomalous in oxygen:  $[^{18}\text{O}/^{17}\text{O}] = 5.2$  in the solar system, while

$[^{18}\text{O}/^{17}\text{O}] \sim 4$  (Wouterloot et al. 2008) in the local galaxy. This difference in  $\Delta^{17}\text{O}$  of about 500‰ should be a smoking gun for interstellar origin, but extreme care must be taken to be sure that the signal is not diluted significantly by surrounding aerogel or any embedding medium such as epoxy, particularly as the statistical precision of the measurement will be compromised by small counting statistics. Although isotopic analyses are currently possible on crater residues using existing techniques, low-risk sample preparation techniques for isotopic analysis of particles in aerogel will require substantial development.

*Acknowledgments*—This manuscript was improved due to the thoughtful comments of Joe Nuth, Sean Brennan, and John Bradley.

*Editorial Handling*—Dr. John Bradley

## REFERENCES

- Bechtel H. A., Flynn G., Allen C., Anderson D., Ansari A., Bajt S., Bastien R. S., Bassim N., Borg J., Brenker F. E., Bridges J., Brownlee D. E., Burchell M., Burghammer M., Butterworth A. L., Changela H., Cloetens P., Davis A. M., Doll R., Floss C., Frank D., Gainsforth Z., Grün E., Heck P. R., Hillier J. K., Hoppe P., Hudson B., Huth J., Hvide B., Kearsley A., King A. J., Lai B., Leitner J., Lemelle L., Leroux H., Leonard A., Lettieri R., Marchant W., Nittler L. R., Oglione R., Ong W. J., Postberg F., Price M. C., Sandford S. A., Tresseras J. S., Schmitz S., Schoonjans T., Silversmit G., Simionovici A., Solé V. A., Srama R., Stephan T., Sterken V., Stodolna J., Stroud R. M., Sutton S., Trieloff M., Tsou P., Tsuchiyama A., Tyliczszak T., Vekemans B., Vincze L., Korff J. V., Westphal A. J., Wordsworth N., Zevin D., Zolensky M. E., and >30,000 Stardust@home dusters. 2014. Preliminary Examination III: Infrared spectroscopic analysis of interstellar dust candidates. *Meteoritics and Planetary Science*, doi:10.1111/maps.12125.
- Brenker F. E., Schoonjans T., Silversmit G., Vekemans B., Vincze L., Westphal A. J., Allen C., Anderson D., Ansari A., Bajt S., Bastien R. S., Bassim N., Bechtel H. A., Borg J., Bridges J., Brownlee D. E., Burchell M., Burghammer M., Butterworth A. L., Changela H., Cloetens P., Davis A. M., Doll R., Floss C., Flynn G., Fougeray P., Frank D., Gainsforth Z., Grün E., Heck P. R., Hillier J. K., Hoppe P., Hudson B., Huth J., Hvide B., Kearsley A., King A. J., Lai B., Leitner J., Lemelle L., Leroux H., Leonard A., Lettieri R., Marchant W., Nittler L. R., Oglione R., Ong W. J., Postberg F., Price M. C., Sandford S. A., Sans Tresseras J., Schmitz S., Simionovici A., Solé V. A., Srama R., Stephan T., Sterken V., Stodolna J., Stroud R. M., Sutton S., Trieloff M., Tsou P., Tsuchiyama A., Tyliczszak T., Korff J. V., Wordsworth N., Zevin D., Zolensky M. E., and >30,000 Stardust@home dusters. 2014. Stardust Interstellar Preliminary Examination V: X-ray fluorescence analysis of interstellar candidates at ID13. *Meteoritics and Planetary Science*, doi:10.1111/maps.12206.
- Butterworth A. L., Westphal A. J., Tyliczszak T., Gainsforth Z., Stodolna J., Frank D., Allen C., Anderson D., Ansari A., Bajt S., Bastien R. S., Bassim N., Bechtel H. A., Borg J., Brenker F. E., Bridges J., Brownlee D. E., Burchell M., Burghammer M., Butterworth A. L., Changela H., Cloetens P., Davis A. M., Doll R., Floss C., Flynn G., Grün E., Heck P. R., Hillier J. K., Hoppe P., Hudson B., Huth J., Hvide B., Kearsley A., King A. J., Lai B., Leitner J., Lemelle L., Leroux H., Leonard A., Lettieri R., Marchant W., Nittler L. R., Oglione R., Ong W. J., Postberg F., Price M. C., Sandford S. A., Sans Tresseras J., Schmitz S., Schoonjans T., Silversmit G., Simionovici A., Solé V. A., Srama R., Stephan T., Sterken V., Stodolna J., Stroud R. M., Sutton S., Trieloff M., Tsou P., Tsuchiyama A., Tyliczszak T., Vekemans B., Vincze L., Korff J. V., Wordsworth N., Zevin D., Zolensky M. E., and >30,000 Stardust@home dusters. 2014. Stardust Interstellar Preliminary Examination IV: Scanning transmission X-ray analysis of major rock-forming elements in interstellar dust candidates. *Meteoritics and Planetary Science*, doi:10.1111/maps.12220.
- Draine B. 2009. Perspectives on interstellar dust inside and outside the heliosphere. *Space Science Reviews* 143:333–345.
- Flynn G., Sutton S., Lai B., Wirick S., Allen C., Anderson D., Ansari A., Bajt S., Bastien R. S., Bassim N., Bechtel H. A., Borg J., Brenker F. E., Bridges J., Brownlee D. E., Burchell M., Burghammer M., Butterworth A. L., Changela H., Cloetens P., Davis A. M., Doll R., Floss C., Frank D., Gainsforth Z., Grün E., Heck P. R., Hillier J. K., Hoppe P., Hudson B., Huth J., Hvide B., Kearsley A., King A. J., Leitner J., Lemelle L., Leroux H., Leonard A., Lettieri R., Marchant W., Nittler L. R., Oglione R., Ong W. J., Postberg F., Price M. C., Sandford S. A., Tresseras J. S., Schmitz S., Schoonjans T., Silversmit G., Simionovici A., Solé V. A., Srama R., Stephan T., Sterken V., Stodolna J., Stroud R. M., Trieloff M., Tsou P., Tsuchiyama A., Tyliczszak T., Vekemans B., Vincze L., Korff J. V., Westphal A. J., Wordsworth N., Zevin D., Zolensky M. E., and >30,000 Stardust@home dusters. 2014. Stardust Interstellar Preliminary Examination VII: X-ray fluorescence analysis of interstellar candidates at 2-ID-D. *Meteoritics and Planetary Science*, doi:10.1111/maps.12144.
- Frank D., Westphal A. J., Zolensky M. E., Bastien R. K., Gainsforth Z., Allen C., Anderson D., Ansari A., Bajt S., Bassim N., Bechtel H. A., Borg J., Brenker F. E., Bridges J., Brownlee D. E., Burchell M., Burghammer M., Butterworth A. L., Changela H., Cloetens P., Davis A. M., Doll R., Floss C., Flynn G., Grün E., Heck P. R., Hillier J. K., Hoppe P., Hudson B., Huth J., Hvide B., Kearsley A., King A. J., Lai B., Leitner J., Lemelle L., Leroux H., Leonard A., Lettieri R., Marchant W., Nittler L. R., Oglione R., Ong W. J., Postberg F., Price M. C., Sandford S. A., Tresseras J. S., Schmitz S., Schoonjans T., Silversmit G., Simionovici A., Solé V. A., Srama R., Stephan T., Sterken V., Stodolna J., Stroud R. M., Sutton S., Trieloff M., Tsou P., Tsuchiyama A., Tyliczszak T., Vekemans B., Vincze L., Korff J. V., Wordsworth N., Zevin D., and >30,000 Stardust@home dusters. 2013. Stardust Interstellar Preliminary Examination II: Curating the Stardust interstellar dust collector: Picokeystones, the Stardust Interstellar Preliminary Examination (ISPE), and beyond. *Meteoritics and Planetary Science*, doi:10.1111/maps.12147.
- Frisch P. C. and Slavin J. D. 2006. Short-term variations in the galactic environment of the sun. In *Solar journey: The significance of our galactic environment for the heliosphere*

- and earth, edited by Frisch P. C. Dordrecht, the Netherlands: Springer. p. 133.
- Frisch P. C. and Slavin J. D. 2013. <http://arxiv.org/abs/1205.4017v1>. Accessed October 23, 2013.
- Frisch P. C., Dorschner J. M., Geiss J., Greenberg J. M., Gruen E., Landgraf M., Hoppe P., Jones A. P., Kraetschmer W., Linde T., Morfill G., Reach W., Slavin J., Svestka J., Witt A. N., and Zank G. P. 1999. Dust in the local interstellar wind. *The Astrophysical Journal* 525:492.
- Frisch P. C., Redfield S., and Slavin J. D. 2012. The interstellar medium surrounding the sun. *Annual Review of Astronomy and Astrophysics* 49:237–279.
- Gainsforth Z., Brenker F. E., Burghammer M., Simionovici A., Schmitz S., Cloetens P., Lemelle L., Sans Tresseras J., Schoonjans T., Silversmit G., Solé V. A., Vekemans B., Vincze L., Westphal A. J., Allen C., Anderson D., Ansari A., Bajt S., Bastien R. S., Bassim N., Bechtel H. A., Borg J., Bridges J., Brownlee D. E., Burchell M., Butterworth A. L., Changela H., Davis A. M., Doll R., Floss C., Flynn G., Frank D., Grün E., Heck P. R., Hillier J. K., Hoppe P., Hudson B., Huth J., Hvide B., Kearsley A., King A. J., Lai B., Leitner J., Leroux H., Leonard A., Lettieri R., Marchant W., Nittler L. R., Oglione R., Ong W. J., Postberg F., Price M. C., Sandford S. A., Srama R., Stephan T., Sterken V., Stodolna J., Stroud R. M., Sutton S., Trieloff M., Tsou P., Tsuchiyama A., Tyliczszak T., Korff J. V., Wordsworth N., Zevin D., Zolensky M. E., and >30,000 Stardust@home dusters. 2014. Stardust Interstellar Preliminary Examination VIII: X-ray diffraction analysis of interstellar candidates. *Meteoritics and Planetary Science*, doi:10.1111/maps.12148.
- Gehrels N. 1986. Confidence limits for small numbers of events in astrophysical data. *The Astrophysical Journal* 303:336.
- Grün E., Zook H. A., Baguhl M., Balogh A., Bame S. J., Fechtig H., Forsyth R., Hanner M. S., Horanyi M., Kissel J., Lindblad B.-A., Linkert D., Linkert G., Mann I., McDonnell J. A. M., Morfill G. E., Phillips J. L., Polansky C., Schwehm G., Siddique N., Staubach P., Svestka J., and Taylor A. 1993. Discovery of Jovian dust streams and interstellar grains by the ULYSSES spacecraft. *Nature* 362:428.
- Grün E., Baguhl M., Divine N., Fechtig H., Hamilton D. P., Hanner M. S., Kissel J., Lindblad B.-A., Linkert D., Linkert G., Mann I., McDonnell J. A. M., Morfill G. E., Polansky C., Riemann R., Schwehm G., Siddique N., Staubach P., and Zook H. A. 1995. Three years of Galileo dust data. *Planetary and Space Science* 43:953–969.
- Krüger H., Altobelli N., Anweiler B., Dermott S. F., Dikarev V., Graps A. L., Grün E., Gustafson B. A., Hamilton D. P., Hanner M. S., Horny M., Kissel J., Landgraf M., Lindblad B. A., Linkert D., Linkert G., Mann I., McDonnell J. A. M., Morfill G. E., Polansky C., Schwehm G., Srama R., and Zook H. A. 2006. Five years of Ulysses dust data: 2000–2004. *Planetary and Space Science* 54:932–956.
- Krüger H., Dikarev V., Anweiler B., Dermott S. F., Graps A. L., Grün E., Gustafson B. A., Hamilton D. P., Hanner M. S., Horny M., Kissel J., Linkert D., Linkert G., Mann I., McDonnell J. A. M., Morfill G. E., Polansky C., Schwehm G., and Srama R. 2010. Three years of Ulysses dust data: 2005 to 2007. *Planetary and Space Science* 58:951–964.
- Landgraf M., Müller M., and Grün E. 2006. Prediction of the in-situ dust measurements of the Stardust mission to comet 81P/Wild 2. *Planetary and Space Science* 47: 1029.
- Meyer D. M., Lauroesch J. T., Peek J. E. G., and Heiles C. 2012. The remarkable high pressure of the local Leo cold cloud. *The Astrophysical Journal*. 752:119.
- Postberg F., Hillier J. K., Armes S. P., Bugiel S., Butterworth A. L., Dupin D., Fielding L. A., Fujii S., Gainsforth Z., Grün E., Li Y. W., Srama R., Sterken V., Stodolna J., Trieloff M., Westphal A. J., Allen C., Anderson D., Ansari A., Bajt S., Bastien R. S., Bassim N., Bechtel H. A., Borg J., Brenker F. E., Bridges J., Brownlee D. E., Burchell M., Burghammer M., Changela H., Cloetens P., Davis A. M., Doll R., Floss C., Flynn G., Frank D., Heck P. R., Hoppe P., Hudson B., Huth J., Hvide B., Kearsley A., King A. J., Lai B., Leitner J., Lemelle L., Leroux H., Leonard A., Lettieri R., Marchant W., Nittler L. R., Oglione R., Ong W. J., Price M. C., Sandford S. A., Tresseras J. S., Schmitz S., Schoonjans T., Silversmit G., Simionovici A., Solé V. A., Stephan T., Stroud R. M., Sutton S., Tsou P., Tsuchiyama A., Tyliczszak T., Vekemans B., Vincze L., Korff J. V., Wordsworth N., Zevin D., Zolensky M. E., and >30,000 Stardust@home dusters. 2014. Stardust Interstellar Preliminary Examination IX: Interstellar dust analog experiments at the Heidelberg Dust Accelerator. *Meteoritics and Planetary Science*, doi:10.1111/maps.12173.
- Simionovici A., Lemelle L., Cloetens P., Solé V. A., Sans Tresseras J., Butterworth A. L., Westphal A. J., Gainsforth Z., Stodolna J., Allen C., Anderson D., Ansari A., Bajt S., Bassim N., Bastien R. S., Bechtel H. A., Borg J., Brenker F. E., Bridges J., Brownlee D. E., Burchell M., Burghammer M., Changela H., Davis A. M., Doll R., Floss C., Flynn G., Frank D., Grün E., Heck P. R., Hillier J. K., Hoppe P., Hudson B., Huth J., Hvide B., Kearsley A., King A. J., Lai B., Leitner J., Leonard A., Leroux H., Lettieri R., Marchant W., Nittler L. R., Oglione R., Ong W. J., Postberg F., Price M. C., Sandford S. A., Schmitz S., Schoonjans T., Schreiber K., Silversmit G., Srama R., Stephan T., Sterken V., Stroud R. M., Sutton S., Trieloff M., Tsou P., Tsuchiyama A., Tyliczszak T., Vekemans B., Vincze L., Korff J. V., Wordsworth N., Zevin D., Zolensky M. E., and >30,000 Stardust@home dusters. 2014. Stardust Interstellar Preliminary Examination VI: X-ray fluorescence analysis of interstellar candidates at ID22. *Meteoritics and Planetary Science*, doi:10.1111/maps.12208.
- Slavin J. D., Frisch P. C., Heerikhuisen J., Pogorelov N. V., Mueller H.-R., Reach W. T., Zank G. P., Dasgupta B., and Avinash K. 2009. Exclusion of tiny interstellar dust grains from the heliosphere arXiv:0911.1492v1, doi:10.1063/1.3396301.
- Sterken V., Westphal A. J., Altobelli N., Grün E., Postberg F., Srama R., Allen C., Anderson D., Ansari A., Bajt S., Bastien R. S., Bassim N., Bechtel H. A., Borg J., Brenker F. E., Bridges J., Brownlee D. E., Burchell M., Burghammer M., Butterworth A. L., Changela H., Cloetens P., Davis A. M., Doll R., Floss C., Flynn G., Frank D., Gainsforth Z., Heck P. R., Hillier J. K., Hoppe P., Hudson B., Huth J., Hvide B., Kearsley A., King A. J., Lai B., Leitner J., Lemelle L., Leroux H., Leonard A., Lettieri R., Marchant W., Nittler L. R., Oglione R., Ong W. J., Price M. C., Sandford S. A., Tresseras J. S.,

- Schmitz S., Schoonjans T., Silversmit G., Simionovici A., Solé V. A., Stephan T., Stodolna J., Stroud R. M., Sutton S., Trierloff M., Tsou P., Tsuchiyama A., Tyliczszak T., Vekemans B., Vincze L., Korff J. V., Wordsworth N., Zevin D., Zolensky M. E., and > 30,000 Stardust@home dusters. 2014. Stardust Interstellar Preliminary Examination X: Propagation of interstellar dust in the heliosphere: application to Stardust. *Meteoritics and Planetary Science*, doi:10.1111/maps.12219.
- Stroud R. M., Allen C., Anderson D., Ansari A., Bajt S., Bassim N., Bastien R. S., Bechtel H. A., Borg J., Brenker F. E., Bridges J., Brownlee D. E., Burchell M., Burghammer M., Butterworth A. L., Changela H., Cloetens P., Davis A. M., Doll R., Floss C., Flynn G., Frank D., Gainsforth Z., Grün E., Heck P. R., Hillier J. K., Hoppe P., Huth J., Hvide B., Kearsley A., King A. J., Lai B., Leitner J., Lemelle L., Leroux H., Leonard A., Lettieri R., Marchant W., Nittler L. R., Oglione R., Ong W. J., Postberg F., Price M. C., Sandford S. A., Sans Tresseras J., Schmitz S., Schoonjans T., Silversmit G., Simionovici A., Solé V. A., Srama R., Stephan T., Sterken V., Stodolna J., Sutton S., Trierloff M., Tsou P., Tsuchiyama A., Tyliczszak T., Vekemans B., Vincze L., Korff J. V., Westphal A. J., Zevin D., Zolensky M. E., and > 30,000 Stardust@home dusters. 2014. Stardust Interstellar Preliminary Examination XI: Analysis of impacts in Stardust Interstellar Foils. *Meteoritics and Planetary Science*, doi:10.1111/maps.12136.
- Tsou P., Brownlee D. E., Sandford S. A., Hörz F., and Zolensky M. E. 2003. Wild 2 and interstellar sample collection and Earth return. *Journal of Geophysical Research* E108:8113.
- Westphal A. J., Anderson D., Butterworth A. L., Frank D., Hudson B., Lettieri R., Marchant W., Korff J. V., Zevin D., Ardizzone A., Campanile A., Capraro M., Courtney K., Crumpler D., Cwik R., Gray F. J., Imada G., Karr J., Lau Wan Wah L., Mazzucato M., Motta P. G., Spencer R. C., Woodrough S. B., Santoni I. C., Sperry G., Terry J., Wordsworth N., Yanke T., Sr, Allen C., Ansari A., Bajt S., Bastien R. S., Bassim N., Bechtel H. A., Borg J., Brenker F. E., Bridges J., Brownlee D. E., Burchell M., Burghammer M., Changela H., Cloetens P., Davis A. M., Doll R., Floss C., Flynn G., Gainsforth Z., Grün E., Heck P. R., Hillier J. K., Hoppe P., Huth J., Hvide B., Kearsley A., King A. J., Lai B., Leitner J., Lemelle L., Leroux H., Leonard A., Nittler L. R., Oglione R., Ong W. J., Postberg F., Price M. C., Sandford S. A., Tresseras J. S., Schmitz S., Schoonjans T., Silversmit G., Simionovici A., Solé V. A., Srama R., Stephan T., Sterken V., Stodolna J., Stroud R. M., Sutton S., Trierloff M., Tsou P., Tsuchiyama A., Tyliczszak T., Vekemans B., Vincze L., Zolensky M. E., and > 30,000 Stardust@home dusters. 2014. Stardust Interstellar Preliminary Examination I: Identification of interstellar candidates. *Meteoritics and Planetary Science*, doi:10.1111/maps.12168.
- Wouterloot J. G. A., Henkel C., Brand J., and Davis G. R. 2008. Galactic interstellar  $^{18}\text{O}/^{17}\text{O}$  ratios—A radial gradient? *Astronomy & Astrophysics* 487:237–246.
-